

CUT-OFF FREQUENCY AND DOMINANT EIGENFUNCTION COMPUTATION IN COMPLEX DIELECTRIC GEOMETRIES VIA DOMSKER-KAČ FORMULA AND MONTE CARLO METHOD

V. Galdi, V. Pierro, and I. M. Pinto
D.I.³.E., University of Salerno
via Ponte Don Melillo
84084 Fisciano (SA), Italy

Abstract

The Donsker-Kač formula can be adapted to compute the dominant eigenvalues and eigenfunctions in dielectric waveguides with complicated geometry, in the weak guidance approximation. The computation of the involved functional (path) integrals is accomplished by means of a reduced-variance Monte Carlo method. The method seems attractive by comparison with standard techniques (Moments Method and Finite Elements) in terms of computational budget.

1 - Introduction

The computation of dominant eigenvalues and eigenfunctions is a key problem in guided wave theory. Unfortunately, analytic solutions exist only whenever Helmholtz equation is solvable (separable) in the given geometry. Whenever the transverse geometry is complex and/or the waveguide is filled with an inhomogeneous medium with complicated refraction index profile, one must resort to numerical methods. The standard choice is Harrington Moments Method or Finite Element Methods. These techniques are relatively expensive in terms of memory and CPU requirements, since they ultimately reduce to the inversion of a large matrix. Furthermore, these techniques were not originally envisaged as a tool for eigenvalues calculation, even if they can be used as such. Conversely, the Donsker-Kač (henceforth DK) method, originally developed in connection with Schrödinger equation, is a general approach for computing eigenvalues, which can be readily rephrased to apply to Helmholtz equation. The only underlying difficulty is related to the peculiar calculus involved: the functional path integral. In this connection, significant advances have been made in recent times, which make the DK formula an attractive alternative to the usual methods. In this paper we present an algorithm for computing the lowest order eigenvalue and eigenfunction in dielectric waveguides with general cross-section geometry and general transverse refraction index distributions, based on Donsker-Kač formula and reduced-variance Monte Carlo methods. The paper is organized as follows. In *Section 2* we review the DK formula, in connection with Helmholtz

equation. In *Section 3*, we discuss an efficient (fast and accurate) numerical strategy for computing the functional integrals. In *Section 4* we outline a comparison between the proposed method and the std. ones (Method of Moments, Finite Elements) in terms of computational budget. In *Section 5* we present some representative computational results, and compare with some known exact solutions. Conclusions follow under *Section 6*. The functional integral concept and the boundary value problems used to make computations are presented in the Appendixes.

2 - The Donsker-Kač Formula

Let:

$$L_x = \nabla^2 - V(x), \quad x \in R^n \quad (1)$$

a second order differential operator, where $V(x)$ is continuous and bounded from below. We assume that L_x has a discrete spectrum of real eigenvalues [1], $\lambda_1 < \lambda_2 < \lambda_3 < \dots$, and associated eigenfunctions ϕ_j , $j = 1, 2, \dots$ forming an orthonormal basis in $L^2(R^n)$ [2] and satisfying the following elliptic boundary value problem with regularity condition at infinity:

$$\nabla^2 \phi - (V - \lambda)\phi = 0. \quad (2)$$

It is well known that the *associated parabolic* equation

$$\frac{\partial \psi}{\partial t} = \nabla^2 \psi(x, t) - V(x)\psi(x, t), \quad t \in R \quad (3)$$

with initial condition:

$$\psi(x, 0) = \delta(x - x_0) \quad (4)$$

and regularity condition at infinity, admits the following (exact) solution [3], [4]:

$$\psi(x_0, 0; x, t) = E_{(x_0, 0; x, t)} \left[\exp \left\{ - \int_0^t V[w(\tau)] d\tau \right\} \right], \quad (5)$$

where $E_{(x_0, 0; x, t)}$ is a *conditioned* Wiener functional integral (see *Appendix A*), over all (Wiener) paths originating from $w(0) = x_0$ and ending at $w(t) = x$. On the other hand, eq.s (3), (4) admit the equivalent solution [3]:

$$\psi(x_0, 0; x, t) = \sum_{j=1}^{\infty} e^{-\lambda_j t} \phi_j(x) \phi_j^*(x_0). \quad (6)$$

By comparing eq. (6) to (5), one readily finds that [5]:

$$\begin{aligned} \lambda_1 &\sim (t_2 - t_1)^{-1} \log \left[\frac{\psi(x_0, 0; x, t_1)}{\psi(x_0, 0; x, t_2)} \right] = \\ &= (t_2 - t_1)^{-1} \log \left[\frac{E_{(x_0, 0; x, t_1)} \left[\exp \left\{ - \int_0^{t_1} V[w(\tau)] d\tau \right\} \right]}{E_{(x_0, 0; x, t_2)} \left[\exp \left\{ - \int_0^{t_2} V[w(\tau)] d\tau \right\} \right]} \right], \quad t_2 > t_1, \quad (7) \end{aligned}$$

$$\phi_1(x) \sim C \psi(x_0, 0, x, t) = C E_{(x_0, 0; x, t)} \left[\exp \left\{ - \int_0^t V[w(\tau)] d\tau \right\} \right], \quad (8)$$

where C is a normalization constant and the equality holds for $t, t_1, t_2 \rightarrow \infty$.

The error $\epsilon_{DK}(\lambda_1)$ affecting eq. (7) can be estimated by combining the logarithmic counterpart of eq. (6) at two different times t_1, t_2 , whence [5]:

$$\epsilon_{DK}(\lambda_1) = (t_2 - t_1)^{-1} \left| \log \left\{ \frac{1 + \sum_{j>1} e^{-(\lambda_j - \lambda_1)t_1} \frac{\phi_j(x)\phi_j^*(x_0)}{\phi_1(x)\phi_1^*(x_0)}}{1 + \sum_{j>1} e^{-(\lambda_j - \lambda_1)t_2} \frac{\phi_j(x)\phi_j^*(x_0)}{\phi_1(x)\phi_1^*(x_0)}} \right\} \right|. \quad (9)$$

This shows that the error can be made in principle as small as one wishes by choosing t_1, t_2 large enough, under the assumption of a strictly increasing eigenvalues sequence. In practice, values of t less than ten proved to be adequate for all practical purposes, in all simulations we made. Similar results hold for eq. (8) as well.

The DK method as expounded above, applies provided the spectrum of L_x is bounded from below, left-discrete, and possibly including a continuous part [1], as in all guided-wave propagation problems.

3 - Implementation

The Wiener functional integrals involved in (7), (8) can be computed without any restriction on $V(x)$ using Monte Carlo methods [6]-[7].

In this section we address the general problem of computing the Wiener functional integral (expectation value) of a regular functional $g[x(\cdot), t]$. In our special case we have:

$$g[x(\cdot), t] = \exp \left\{ - \int_0^t V[x(\tau)] d\tau \right\}. \quad (10)$$

The underlying idea can be explained as follows. As a first step we introduce a set of $N + 1$ discrete equispaced times $\tau_0 = 0$ to $\tau_N = t$, with $\tau_{k+1} - \tau_k = \Delta$, and associated vectors (points) $x(\tau_k) = x_k \in R^n$, $k = 0, 1, \dots, N$. Hence:

$$\begin{aligned} E_{(x_0, 0; x, t)} \{g[x(\cdot), t]\} &= \lim_{N \rightarrow \infty} E_{(x_0, 0; x, t)} \{g[\hat{x}_N(\cdot), t]\} = \\ &= \lim_{N \rightarrow \infty} E_{(x_0, 0; x, t)} \{\hat{g}_N(x_0, \mathbf{x}, x_N)\} = \\ &= \lim_{N \rightarrow \infty} \int_{[R^n]^{N-1}} F(x_0, \mathbf{x}, x_N) d\mu(\mathbf{x}), \end{aligned} \quad (11)$$

where $\hat{x}_N(t)$ is a piecewise linear path with (fixed) end points x_0, x_N going through x_1, \dots, x_{N-1} , \mathbf{x} is the $N - 1$ -dimensional vector $\{x_1, \dots, x_{N-1}\}$, for which the functional $g[x(\cdot), t]$ becomes the function \hat{g}_N ,

$$F(x_0, \mathbf{x}, x_N) = \hat{g}_N(x_0, \mathbf{x}, x_N) \prod_{k=1}^N p(x_{k-1}, \tau_{k-1}; x_k, \tau_k), \quad (12)$$

represents the value of $g[x(\cdot), t]$ on \hat{x}_N weighted by the probability of the path \hat{x}_N regarded as generated by a Wiener process with transition probability $p(x', t'; x, t)$ (see *Appendix A*), and $d\mu(\mathbf{x}) = dx_1 \dots dx_{N-1}$.

The next step is to resort to a fundamental property of the Monte Carlo method which can be established as follows. For *any* function $D(x_0, \mathbf{x}, x_N)$ such that $D(\cdot)d\mu(\mathbf{x})$ is an exact differential, $d\nu(\mathbf{x})$ one has:

$$E_{(x_0, 0; x, t)} \{g[x(\cdot), t]\} = \lim_{N \rightarrow \infty} \int_{[R^n]^{N-1}} \frac{F(x_0, \mathbf{x}, x_N)}{D(x_0, \mathbf{x}, x_N)} d\nu(\mathbf{x}), \quad (13)$$

which can be interpreted by saying that the sought (conditioned) expectation value of the functional is (the limit of) the average of the function F/D of a stochastic vector \mathbf{x} generated with statistical density $D(x_0, \mathbf{x}, x_N)$ [6], [8].

Thus, we can compute the Wiener functional integral (13) using the arithmetic means:

$$\mu_{M,N}^{(1)} = M^{-1} \sum_{h=1}^M \frac{F(x_0, \mathbf{x}_h, x_N)}{D(x_0, \mathbf{x}_h, x_N)}, \quad (14)$$

where \mathbf{x}_h is a random vector generated with statistical density $D(x_0, \mathbf{x}_h, x_N)$. Hence:

$$\begin{aligned} E_{(x_0, 0; x, t)} \{g[x(\cdot), t]\} &= \lim_{N \rightarrow \infty} E_{(x_0, 0; x, t)} \{\hat{g}_N(x_0, \mathbf{x}, x_N)\} = \\ &= \lim_{N \rightarrow \infty} \lim_{M \rightarrow \infty} \mu_{M,N}^{(1)}. \end{aligned} \quad (15)$$

Obviously, for any finite N and M the result will be affected by *i*) a systematic error due to the effect of discretization (average over piecewise linear paths instead of general paths), viz.:

$$\epsilon_{sys}(N) = E \{g[x(\cdot), t]\} - E \{\hat{g}(x_0, \mathbf{x}, x_N)\}, \quad (16)$$

which is a function of N alone and vanishes as $N \rightarrow \infty$, and *ii*) a statistical error, which in view of the central limit theorem is asymptotically gaussian, with zero average and r.m.s. deviation:

$$\epsilon_{stat}(M, N) \sim \left\{ M^{-1} \text{var} \left[\frac{F(x_0, \mathbf{x}, x_N)}{D(x_0, \mathbf{x}, x_N)} \right] \right\}^{1/2}, \quad (17)$$

which depends (weakly) on N , as well as (strongly) on M . It is now convenient to capitalize on the freedom in the choice of $D(\cdot)$ to reduce the variance of the estimator by acting on the variance of F/D in (17).

A very good tradeoff between power and ease is possibly supplied by the so-called *importance sampling technique* [6], [8], for which:

$$D(x_0, \mathbf{x}, x_N) = \prod_{i=1}^{N-1} D_i(x_i), \quad (18)$$

with:

$$D_i(x_i) = \frac{p(x_{i-1}, \tau_{i-1}; x_i, \tau_i) p(x_i, \tau_i; x_N, \tau_N)}{p(x_{i-1}, \tau_{i-1}; x_N, \tau_N)}. \quad (19)$$

It can be proved that $D_i(x_i)$ is a normal distribution [6] with mean and covariance¹

$$E(x_i) = x_{i-1} \frac{\tau_N - \tau_i}{\tau_N - \tau_{i-1}} + x_N \frac{\tau_i - \tau_{i-1}}{\tau_N - \tau_{i-1}}, \quad (20)$$

$$\sigma^2(x_i) = 2 \frac{(\tau_N - \tau_i)(\tau_i - \tau_{i-1})}{\tau_N - \tau_{i-1}}. \quad (21)$$

Letting eq.s (18), (19) into (13), and taking (12) into account, it is concluded that:

$$\frac{F(x_0, \mathbf{x}, x_N)}{D(x_0, \mathbf{x}, x_N)} = \hat{g}_N(x_0, \mathbf{x}, x_N) p(x_0, 0; x, t). \quad (22)$$

Let us thus summarize the main steps for computing the functional integrals in (7), (8), where the functional $g[(\cdot), t]$ is given by (10):

step 1: path generation using the density $D(x_0, \mathbf{x}, x_N)$ given by (18),(19);

step 2: numerical evaluation of:

$$\frac{F(x_0, \mathbf{x}, x_N)}{D(x_0, \mathbf{x}, x_N)} = p(x_0, 0; x, t) \exp \left\{ -\Delta \left[\sum_{k=0}^N V(x_k) - \frac{1}{2} [V(x_0) + V(x_N)] \right] \right\};$$

(the stochastic trapezoidal rule used above implies a systematic error $\mathcal{O}(\Delta^2)$ [6]);

step 3: evaluation of the moments:

$$\mu_{M,N}^{(1)} = M^{-1} \sum_{h=1}^M \frac{F(x_0, \mathbf{x}_h, x_N)}{D(x_0, \mathbf{x}_h, x_N)},$$

$$\mu_{M,N}^{(2)} = M^{-1} \sum_{h=1}^M \left[\frac{F(x_0, \mathbf{x}_h, x_N)}{D(x_0, \mathbf{x}_h, x_N)} \right]^2,$$

needed to compute the functional integral (10) using (13), and the confidence interval of the estimation:

$$\delta_{M,N} = \mu_{M,N}^{(1)} \pm \alpha M^{-1/2} (\mu_{M,N}^{(2)} - \mu_{M,N}^{(1)2})^{1/2}, \quad (23)$$

where α depends on the sought confidence level;

step 4: evaluation of the discretization and statistical errors in computing formulas (7), (8), using standard error propagation formulas.

¹Note that since, as already stated, $x_i \in \mathbb{R}^n, \forall i$, then E and σ^2 are a vector-mean, and (diagonal) coherency matrix.

4 - Comparison with Other Methods

In this section we outline a comparison between our DK-Monte Carlo method (henceforth DKMC) and other standard techniques like Method of Moments and Finite Elements Method (in the following referred as MoM and FEM) to compute eigenvalues, in terms of computational budget. The main (nice) differences between DKMC and MoM/FEM can be summarized as follows:

- DKMC accomodates quite naturally the regularity-at-infinity boundary conditions which are typical of *open* structures. FEM and MoM, on the other hand, require to impose suitable approximate (e.g., absorbing) b.c.
- DKMC has very mild memory requirements, irrespective of the size $\mathcal{N} \sim \rho/\lambda$ of the problem, ρ being a typical length. In contrast, MoM and FEM require the storage of a large (block-Toeplitz) matrix, and thus require $\sim \mathcal{N}^\alpha$ memory size, $\alpha \in (1, 2)$.
- The computational burden of DKMC goes linearly with *both* problem size *and* embedding dimension n . In MoM and FEM, it grows *more* than linearly w.r. to \mathcal{N} (at fixed n) and exponentially in n (at fixed \mathcal{N}). Note also that DKMC does *not* require any meshing algorithm.
- DKMC is intrinsecally parallelizable.
- Tight accuracy bounds are easily obtained.

On the other hand the main drawback is related to the relatively slow convergency rate ($\propto M^{-1/2}$). As a conclusion, one can state that DKMC is ideal for large (in terms of a wavelength) structures, with complicated geometries and/or constitutive properties, whenever fast computing engines and relatively little memory are available.

5 - Computational Results

To test the accuracy of the method, we consider a circular (longitudinally invariant) dielectric waveguide (optical fiber) with (transverse) refractive index distribution $n^2(x, y) = n_{co}^2[1 - 2Df(x, y)]$ (see *Appendix-B*), in the weak guidance limit.

In *Fig. 1* the exact [9] and DK fundamental (HE_{11}) mode dispersion curves for an infinite-parabolic and step index profile are compared. The computed errors (circles) are displayed in *Fig. 2*, and shown to be much smaller than the corresponding confidence-interval halfwidths (squares) obtained from eq. (23), keeping always within 1%.

As a next example we let the refractive index exhibit a power law dependence. The pertinent HE_{11} DK dispersion curves and (lowest order) eigenfunctions are shown in *Fig. 3* and *4*, respectively.

As a further step in complication, we consider the HE_{11} mode dispersion curve of a finite-width clad waveguide with step and parabolic index profiles shown in *Figs 5, 6*, respectively, where:

$$\eta = \frac{r_{cl}}{r_{co}}, \quad (24)$$

r_{cl} and r_{co} being the clad and core radius, respectively.

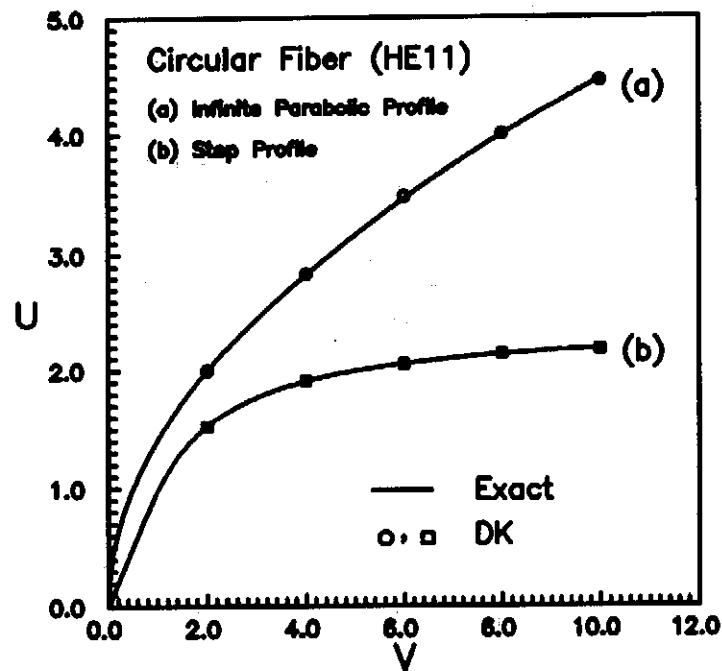


Fig. 1 - Circular fiber. Exact and DK fundamental mode dispersion curves. Infinite parabolic and step index profiles.

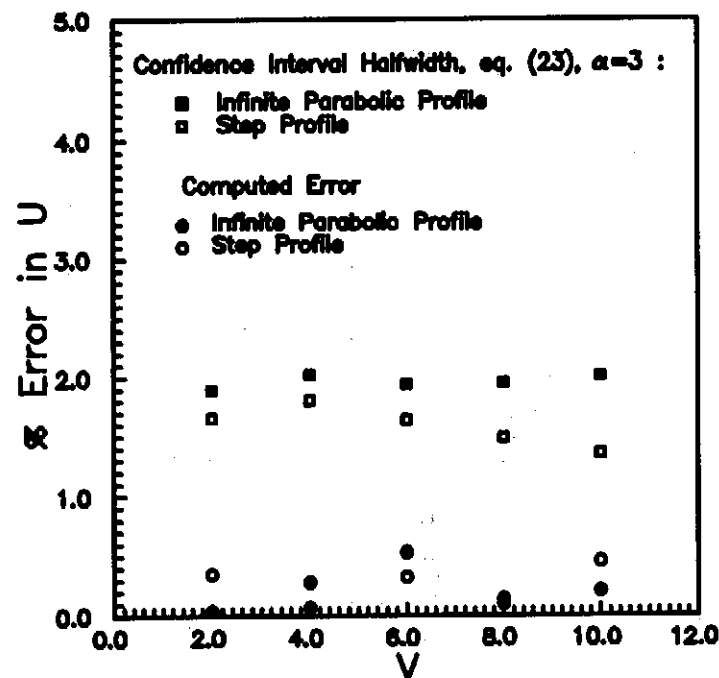


Fig. 2 - Computed errors and estimated confidence interval halfwidths pertinent to Fig. 1.

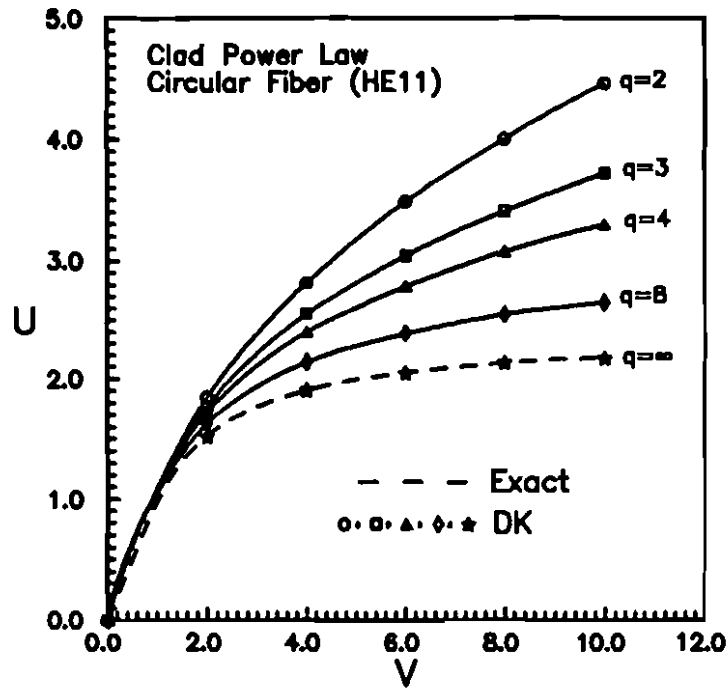


Fig. 3 - Circular fiber. DK fundamental mode dispersion curves.
 Power law index profiles : $f(\bar{R}) = \bar{R}^q [U(\bar{R}) - U(\bar{R} - 1)] + U(\bar{R} - 1)$
 $\bar{R} = (\text{distance from axis})/(\text{core radius})$, $U(\cdot) \equiv \text{Heaviside's function}$.

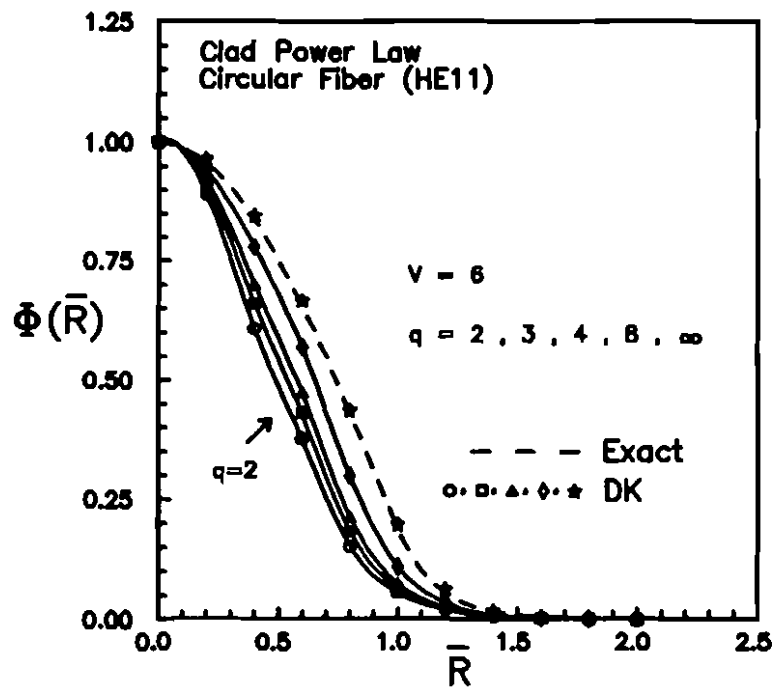


Fig. 4 - DK dominant mode eigenfunctions pertinent to Fig. 3.
 (Mode parameter $V = 6$).

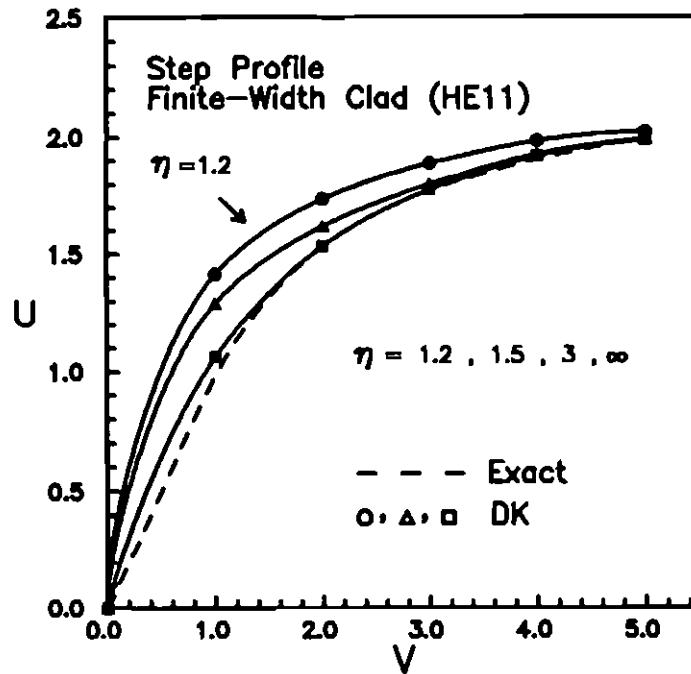


Fig. 5 - Circular fiber with finite width clad. DK fundamental mode dispersion curves. Step index profile : $f(\bar{R}) = U(\bar{R} - 1) + 3U(\bar{R} - \eta)$, $\eta = (\text{clad radius/core radius})$.

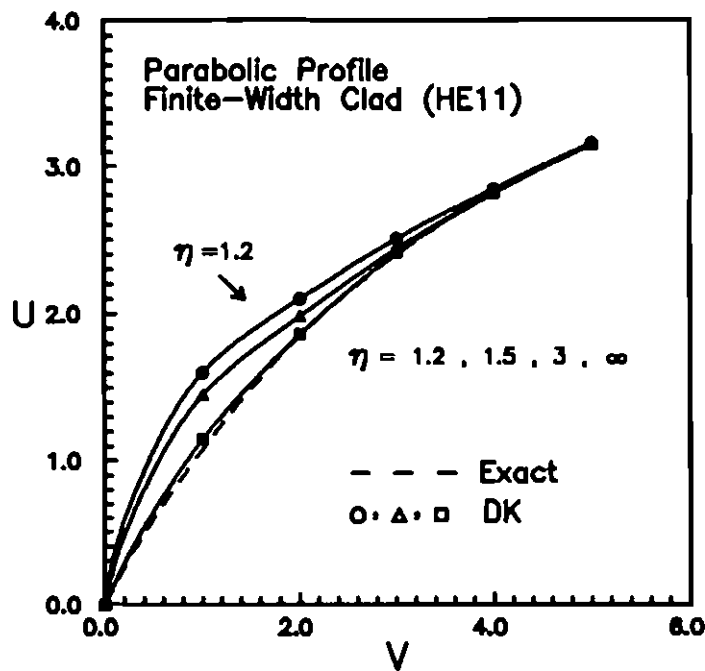


Fig. 6 - Circular fiber with finite width clad. DK fundamental mode dispersion curves. Parabolic index profile : $f(\bar{R}) = \bar{R}^2[U(\bar{R}) - U(\bar{R} - 1)] + U(\bar{R} - 1) + 5U(\bar{R} - \eta)$, $\eta = (\text{clad radius/core radius})$.

The HE_{11} mode dispersion curve of an off-centered core waveguide with a finite-width clad is illustrated in *Fig. 7*, for a step profile index distribution, at various values of

$$\gamma = \frac{\text{offset distance}}{r_{cl} - r_{co}}, \quad 0 \leq \gamma \leq 1 \quad (25)$$

Finally the HE_{11} mode dispersion curve of a step fiber with regular polygonal cross section is shown in *Fig. 8*.

In order to obtain all figures above, a typical number $M \sim 10^4$ paths with $t_1 = 3$, $t_2 = 5$ and $\Delta = t_1/100$ have been used, resulting into a computational time of a few seconds on a RISC workstation. The second eigenvalue can be computed with comparable ease (see [5]). We don't report these results for brevity.

6 - Conclusions and Recommendations

We presented a new method for computing eigenvalues and eigenfuntions in guiding structures. The method is already well-established in different contexts (e.g., quantum mechanics), and appears to be potentially advantageous with respect to both MoM and FEM, as far as its computational budget is concerned, although its convergency features are, in principle, worse.

The method is naturally extended to compute the (lowest order) resonant frequencies in 3D dielectric structures. It can serve as an auxiliary tool in SEM/hybrid modeling as well. It is possible to extend the method to problems involving conducting boundaries, using modified Wiener-paths, featuring absorption or (possibly delayed) reflection to model Dirichlet or Neumann (possibly mixed) boundary conditions [10],[11].

Appendix A - Poor Man's Route to Wiener Path Integral

We define a standard (scalar) Wiener process $w = \{w(t), t \geq 0\}$ originating from x_0 at $t = 0$ as a gaussian process with independent increments such that:

$$w(0) = x_0, \quad E[w(t) - w(s)] = 0, \quad \text{var}[w(t) - w(s)] = 2\mathcal{D}(t - s), \quad t \geq s. \quad (A1)$$

where \mathcal{D} is the so-called *diffusion coefficient*. We can also consider n -dimensional Wiener processes, whose components $\{w_1, w_2, \dots, w_n\}$ are independent scalar Wiener processes with respect to a common family of σ -algebras. It can be shown that the sample paths of a Wiener process are continuous but nowhere differentiable functions of time. The transition probability density:

$$p(x_0, s; x, t) = [4\pi\mathcal{D}(t - s)]^{-1/2} \exp \left[-\frac{(x - x_0)^2}{4\mathcal{D}(t - s)} \right] \quad (A2)$$

satisfies the Fokker-Planck equation:

$$\frac{\partial p}{\partial t} = \mathcal{D} \nabla^2 p. \quad (A3)$$

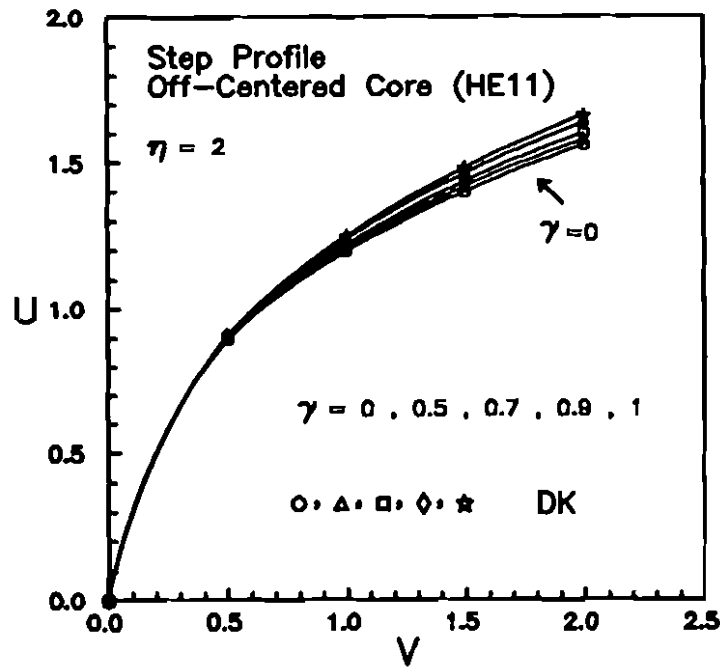


Fig. 7 - Circular fiber with finite width clad and off centered core. DK fundamental mode dispersion curves. Step index profile : $f(\bar{R}, \bar{R}') = U(\bar{R}' - 1) + 5U(\bar{R} - \eta)$, $\bar{R}' = \{[X - \gamma(\eta - 1)]^2 + Y^2\}^{1/2}$, $\gamma = (\text{offset distance})/(\text{clad radius} - \text{core radius})$.

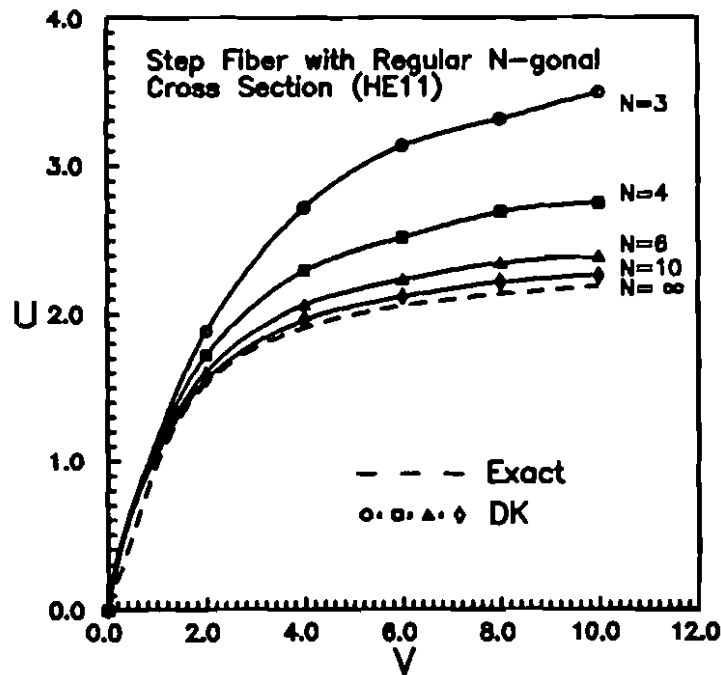


Fig. 8 - Polygonal fiber. DK fundamental mode dispersion curves. Step index profile.

We now introduce a set of $N + 1$ (equispaced) times $t_0 = 0$, $t_N = t$, with $t_k - t_{k-1} = \Delta$, $w(t_k) := x_k$, and a (cylindrical) subset in the space C of continuous functions:

$$K[a_1, b_1, t_1; \dots; a_{N-1}, b_{N-1}, t_{N-1}] = \{w(\cdot) \in C | a_i \leq x_i \leq b_i, \quad i = 1, \dots, N-1\} \subseteq C, \quad (A4)$$

$w(0) = w(t_0) = x_0$ and $w(t) = w(t_N) = x_N$ being fixed. $w(t)$ is called a (conditional) Wiener process, and the following probability defines a measure of the subset K (conditional Wiener measure, [3]):

$$\mu_W[K] = \int_{a_1}^{b_1} \int_{a_2}^{b_2} \dots \int_{a_{N-1}}^{b_{N-1}} p(x_0, t_0; x_1, t_1) p(x_1, t_1; x_2, t_2) \dots p(x_{N-1}, t_{N-1}; x_N, t_N) dx_1 \dots dx_{N-1}. \quad (A5)$$

Wiener was able to demonstrate that, for a wide class of regular functionals $g[w(\cdot), t]$ in the space C of continuous functions in $[0, t]$ with $w(0) = x_0$ and $w(t) = x_N$ fixed, there exists an integral over the measure (A5).

This latter is computed by introducing the piecewise linear paths $\hat{w}_N(t)$ going through $(x_0, t_0) \dots (x_N, t_N)$ for which the functional $g[w(\cdot), t]$ becomes a function $\hat{g}_N(x_0, \mathbf{x}, x_N)$, where $\mathbf{x} = \{x_1, \dots, x_{N-1}\}$, as follows:

$$\int_C g[w(\cdot), t] d_W \mathbf{x} = \lim_{N \rightarrow \infty} (4\pi\mathcal{D}\Delta)^{-N/2} \int_{-\infty}^{\infty} dx_1 \int_{-\infty}^{\infty} dx_2 \dots \int_{-\infty}^{\infty} dx_{N-1} \hat{g}_N(x_0, \mathbf{x}, x_N) \cdot \exp \left\{ - \sum_{s=0}^{N-1} \frac{(x_{s+1} - x_s)^2}{4\mathcal{D}\Delta} \right\}, \quad (A6)$$

where $d_W \mathbf{x}$ is the (conditional) Wiener measure. It is understood [4] that eq. (A6) describes an *average* of the functional over the (conditional) Wiener paths w_N .

Appendix B - Eigenvalue Problems for Dielectric Waveguides

The time-harmonic electromagnetic field in a longitudinally homogeneous cylindrical dielectric waveguide with arbitrary cross section and general refractive index distribution, can be decomposed into a superposition of a finite number of bounded (source-free) modes, plus a (continuous) infinity of leaky modes. In view of the translational invariance of the waveguide, the modal-fields are separable, and we have for the forward and backward propagating modes:

$$\tilde{E}_{\mathbf{q}}^{\pm}(x, y, z) = \tilde{e}(x, y) e^{\mp j\beta_{\mathbf{q}} z}, \quad (B1)$$

$$\tilde{H}_{\mathbf{q}}^{\pm}(x, y, z) = \tilde{h}(x, y) e^{\mp j\beta_{\mathbf{q}} z}, \quad (B2)$$

where $\beta_{\mathbf{q}}$ is the modal propagation constant, \mathbf{q} being the modal index array, which will be henceforth suppressed.

Let us assume the (transverse) refractive index distribution to be described by:

$$n^2(x, y) = n_{co}^2[1 - 2Df(x, y)], \quad (B3)$$

where D is the so called profile height parameter defined by:

$$D = \frac{1}{2} \left[1 - \left(\frac{n_{cl}}{n_{co}} \right)^2 \right], \quad (B4)$$

where n_{co} , n_{cl} are the maximum core and minimum cladding refractive index (no material dispersion assumed), respectively.

In the weak-guidance approximation $D \ll 1$ [9], the fundamental (hybrid) modes are nearly *TEM*, and one has:

$$\begin{aligned} \vec{E}_t(x, y) &\approx \Phi(x, y) e^{\mp j\beta z} [\hat{u}_x e^{\mp j\delta\beta x} + \hat{u}_y e^{\mp j\delta\beta y}], \\ \vec{H}_t(x, y) &\approx \frac{n_{co}}{\zeta_0} \hat{u}_z \times \vec{E}_t(x, y), \\ e_z(x, y) &\approx j \frac{(2D)^{1/2}}{k_0(n_{co}^2 - n_{cl}^2)^{1/2}} \nabla_t \cdot \vec{e}_t, \\ h_z(x, y) &\approx j \frac{(2D)^{1/2}}{k_0(n_{co}^2 - n_{cl}^2)^{1/2}} \nabla_t \cdot \vec{h}_t, \end{aligned} \quad (B5)$$

where k_0 and ζ_0 are the free-space wavenumber and characteristic impedance, respectively, and:

$$\delta\beta_{x(y)} \approx \frac{(2D)^{3/2}}{4k_0(n_{co}^2 - n_{cl}^2)^{1/2}} \frac{\int_{-\infty}^{\infty} \int_{-\infty}^{\infty} \partial_x(y) \Phi^2(x, y) \partial_x(y) f(x, y) dx dy}{\int_{-\infty}^{\infty} \int_{-\infty}^{\infty} \Phi^2(x, y) dx dy}, \quad (B6)$$

It is expedient to introduce scaled coordinates $(X, Y) = (x/\rho, y/\rho)$, ρ being a suitably defined core half-width, and dimensionless waveguide and modal parameters² (see, e.g., [9]):

$$\begin{aligned} V &= \frac{2\pi\rho}{\lambda} (n_{co}^2 - n_{cl}^2)^{1/2}, \quad U = \rho(k_0^2 n_{co}^2 - \beta^2)^{1/2}, \\ W &= \rho(\beta^2 - k_0^2 n_{cl}^2). \end{aligned} \quad (B7)$$

One is led from Maxwell equations to the following scalar eigenvalue problem³

$$[\nabla_t^2 + U^2 - V^2 f(X, Y)] \Phi(X, Y) = 0. \quad (B8).$$

This equation belongs to the class exploited in *Sect. 1*, and thus the DK formalism can be used to compute the dispersion relation $U = U(V)$ (and hence the cut-off frequency) and the dominant mode. As a technical hint note that, with reference e.g. to the eq. (B8) the path integral:

²Modal cutoff occurs when:

$$W = 0, \quad \text{viz.} \quad U = V$$

Note that for bound modes $0 \leq U < V$ and $0 < W \leq V$, and for leaky modes $U \geq V$.

³Similar equations can be written for circular cross-section waveguides for higher order modes as well ([9], Sect. 13.7).

$$E_{(x_0,0;x,t)} \left[\exp \left\{ -V^2 \int_0^t f[w(\tau)] d\tau \right\} \right] \quad (B9)$$

is affected by an increasingly large discretization error as V becomes larger and larger. To prevent this problem, we rescale the equation as follows:

$$[V^{-1} \nabla_t^2 + V^{-1} U^2 - V f] \Phi = 0, \quad (B10)$$

and compute the *scaled* eigenvalue U^2/V , using a Wiener process with diffusion coefficient V^{-1} to generate the paths. This simple device allows us to keep the DK computation parameters (M, Δ, t_1, t_2) *fixed*, irrespective of the value of V , in order to attain the same accuracy.

Acknowledgements

We thank prof. G. Franceschetti for several illuminating discussions, and dr. A. Fedullo for having introduced us to the DK method. Part of this work has been supported through a CNR grant earned by V. Pierro.

References

- [1] D. Ray, Trans. Am. Math. Soc., **77**, 299, 1954.
- [2] M. Reed, B. Simon, *Methods of Modern Mathematical Physics*, II, Academic Press, New York, 1975.
- [3] I.M. Gelfand, A.M. Yaglom, J. Math. Phys., **1**, 48, 1960.
- [4] L.S. Schulman, *Techniques and Applications of Path Integration*, J. Wiley & Sons, New York, 1981.
- [5] M.D. Donsker, M. Kač, J. Res. NBS., **44**, 551, 1950.
- [6] P.E. Kloeden, E. Platen *Numerical Solution of Stochastic Differential Equations*, Springer, NY, 1991.
- [7] I.M. Sobol, *The Monte Carlo Method*, MIR, Moscow, 1975.
- [8] W.H. Press et al., *Numerical Recipes in C*, Cambridge Un. Press, 1992.
- [9] A.W. Snyder, J.D. Love, *Optical Waveguide Theory*, Chapman & Hall, 1983.
- [10] I.I. Gihman and A.V. Skorohod, *Stochastic Differential Equations*, Springer-Verlag, 1972.
- [11] A. Gerardi, et al., System and Control Lett. **4**, 253, 1984.